JOURNAL OF MATERIALS SCIENCE 28 (1993) 2233–2237

The a.c. equivalent circuit of dielectric materials

S. N. AL-REFAIE, H. S. B. ELAYYAN
Electrical Engineering Section, Faculty of Engineering, Mu'tah University, P.O. Box 7, Mu'tah, Karak, Jordan

An equivalent circuit for dielectrics exhibiting frequency dispersion has been obtained using a new multiple-arc analysis in conjunction with relaxation time distribution (RTD). Subsequently, an equivalent network was derived for a zinc oxide (ZnO)-based ceramic varistor at low electric fields. Reported measurements of ZnO varistor resistivity and permittivity were found to correspond satisfactorily to those obtained from the network over the frequency range 30 Hz–10 MHz. The new methodology is, in principle, applicable to any analysable dielectric data.

1. Introduction

The theory of dielectrics has been developed adequately for a limited number of materials. The dispersion characteristics of these dielectrics with frequency are described in terms of a simple Debye single relaxation approach [1]. However, the majority of dielectrics exhibit a pronounced deviation from the simplified Debye treatment. Among these dielectrics, which are of significant engineering applications, are zinc oxide(ZnO)-based ceramics [2, 3], polymers [4, 5], and metal composites such as LiTi [6, 7], and LiNi [8].

In addition to the attempts made to analyse and understand the anomalous behaviour of dielectrics, considerable effort has also been made to develop equivalent circuits representing their dispersion with frequency [9–11]. For instance, in ZnO varistors a number of circuits has been proposed to account for the dispersion at low as well as high electric fields [3, 12]. However, those circuits reflect a limited range of measured data. Hence, a significant part of the characteristics range is, in fact, irreconcilable with the circuit predictions. The bases adopted in those circuit developments relied mainly in either data fitting over a specified range or describing the behaviour more or less in terms of a single relaxation time. As is evident upon many occasions, the representation of a dielectric constant in the complex plane indicates many relaxation times. This is derived from a single circular arc relation in the plane, in comparison to a semicircle for a single relaxation time [13]. Recently, one of the authors has developed a relaxation time distribution formula for dielectrics exhibiting double arcs in the complex plane [14]. This has been extended further to treat multiple-arc relations whereby a generalized formula has been presented [15]. The new approach has been applied in analysing the data of zinc oxide and polydiacetylene dielectrics [16]. This paper reports the use of multiple-arc analysis together with the RTD function in deriving equivalent circuits for dielectrics. While the method developed here is, in principle, applicable to any analysable data, the paper is confined to the example of network derivation for ZnO varistors at low electric fields.

2. Dielectric dispersion relations

Dielectric constants are generally expressed as complex quantities; $\varepsilon^* = \varepsilon' - j\varepsilon''$. ε' and ε'' represent, respectively, the charging and loss components that are functions of frequency. In the ε''–ε' complex plane, the frequency dependence describes a semi-circular locus for the system with a single relaxation time. However, dielectrics exhibiting circular arcs are characterized by many relaxation times with ε^*, for an arc, taking the form [17]

$$\varepsilon^* = \varepsilon_\infty + \frac{\varepsilon_s - \varepsilon_\infty}{1 + (j\omega\tau_0)^{1-\alpha}} \quad (1)$$

The imaginary part of ε^*, which is relevant to the present work, is given as

$$\varepsilon'' = \frac{\frac{1}{2}(\varepsilon_s - \varepsilon_\infty)\cos(\alpha\pi/2)}{\cosh(1-\alpha)S + \sin(\alpha\pi/2)} \quad (2)$$

with $S = \ln(\omega\tau_0)$. ε_s and ε_∞ are the static and high-frequency constants, respectively, α is a constant effectively representing the spread in relaxation times and takes a value between 0 and 1, and τ_0 denotes the most probable relaxation time. The corresponding RTD function takes the form [13, 17]

$$f(u) = \frac{1}{2\pi} \frac{\sin(\alpha\pi)}{\cosh(1-\alpha)u - \cos(\alpha\pi)} \quad (3)$$

with

$$\int_{-\infty}^{\infty} f(u)\,du = 1 \quad (4)$$

where $u = \ln(\tau/\tau_0)$.

With $\alpha = 0$, Equations 1 and 2 reduce to the well-known Debye expressions for the dielectric constant, whilst Equation 3 reduces to the Dirac delta function representing single relaxation time [15, 18].

0022–2461

The distribution function given by Equation 3 has recently been extended by one of the authors, to a relation featuring a multiple-arc plot in the ε''–ε' plane [15] whereby $f(u)$ becomes

$$f(u) = C \sum_{n=1}^{m} \frac{(\varepsilon_{sn} - \varepsilon_{\infty n})\sin(\alpha_n \pi)}{\cosh[(1 - \alpha_n)(u + \beta_n)] - \cos(\alpha_n \pi)} \quad (5)$$

with

$$\varepsilon''(\omega) = \sum_{n=1}^{m} \varepsilon_n''(\omega) \quad (6)$$

where $C = 1/[2\pi \sum_{n=1}^{m} (\varepsilon_{sn} - \varepsilon_{\infty n})]$, $\beta_n = \ln(\tau_{o1}/\tau_{on})$, and $u = \ln(\tau/\tau_{o1})$. n designates an arc and m is the number of evaluated arcs over the range of frequency used. Each term in Equation 6 is determined according to Equation 2 using the corresponding parameters ε_s, ε_∞, α and τ_o. If β_n values are widely separated, the distribution function may feature multiple-peak spectra depending on the relative magnitudes of $(\varepsilon_{sn} - \varepsilon_{\infty n})$ as well as α_n values.

3. RTD function and equivalent circuit

For a dispersion relation characterized by a single relaxation time, τ_o, the RTD yields a Dirac delta function [13] at $\tau = \tau_o$ or $u = 0$. The simplest network representation constitutes a series of R–C components with $RC = \tau_o$ in parallel with a high-frequency capacitance, C_∞, as shown in Fig. 1. Such a circuit corresponds adequately to the variation of the parallel resistance and capacitance with frequency. With σ and ε representing the resistive and capacitive elements, respectively, the parallel a.c. conductivity, σ_p, becomes

$$\sigma_p = \frac{\omega^2 \varepsilon \tau}{1 + \omega^2 \tau^2} \quad (7)$$

On the other hand, for relations featuring multiple arcs in the $\varepsilon'' - \varepsilon'$ complex plane, the continuity of the RTD function implies a rather distributed network representation. However, for a realizable network, circuit with discrete lumped components is often regarded as an appropriate practical choice. With the simplified circuit being sought, then the R–C network used for a single relaxation can be employed in a parallel combination of branches [13], each designated by the time constant $\tau_k = \varepsilon_k/\sigma_k$ as depicted in Fig. 2. Meanwhile, recalling the fact that the total area under the $f(u)$ function yields a value of 1, Equation 4, then a branch admittance to the total admittance gives the branch weighting factor. This, in turn, corresponds to

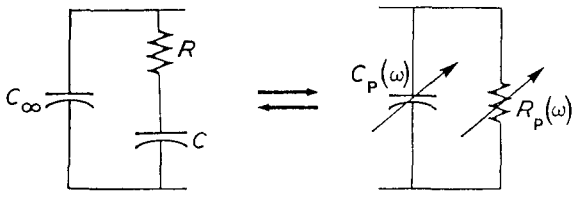

Figure 1 The series R–C circuit and its parallel equivalent representing the semicircular dispersion relation.

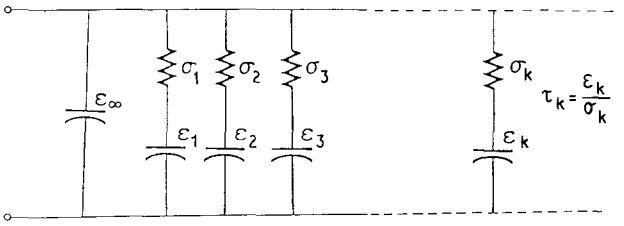

Figure 2 The equivalent circuit representing the circular arc dispersion relation.

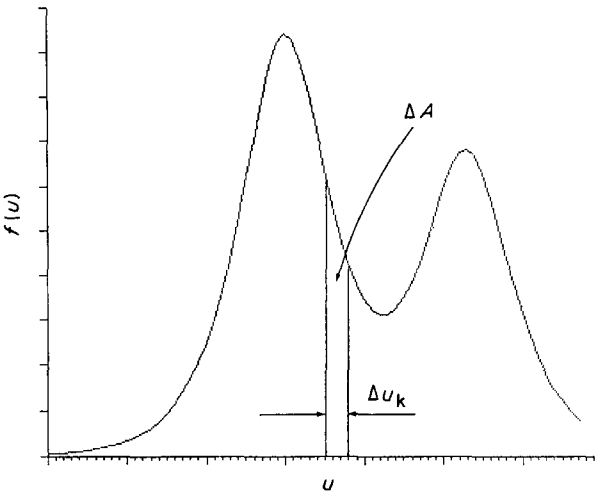

Figure 3 A general RTD function illustrating branch weighting factor ΔA.

the small area, ΔA, under the $f(u)$ function at u_k, as illustrated in Fig. 3, hence

$$\frac{\sigma_k}{\sigma_M} = \Delta A = f(u)\Delta u|_{u=u_k} \quad (8)$$

where σ_M is the measured a.c. conductivity of the dielectric, and σ_k is the conductivity of the branch corresponding to τ_k. The total network conductivity, σ_N, is then

$$\sigma_N = \sum_{1}^{L} \sigma_k \quad (9)$$

with L being the number of branches used. L depends on the effective range in the distribution function $f(u)$, as well as the accuracy of representation judged by comparing σ_N with σ_M. It follows that a branch conductivity, σ_k, becomes

$$\sigma_k = \frac{\omega^2 \varepsilon_k \tau_k}{1 + \omega^2 \tau_k^2} = \sigma_M f(u)\Delta u|_{u=u_k} \quad (10a)$$

or

$$\varepsilon(\tau_k) = \left(\frac{1 + \omega^2 \tau_k^2}{\omega^2 \tau_k}\right) \sigma_M f(u_k)\Delta u_k \quad (10b)$$

with $u_k = \ln(\tau_k/\tau_{o1})$.

Calculation of ε_k enables finding the branch conductivity, σ_k, using the corresponding time constant,

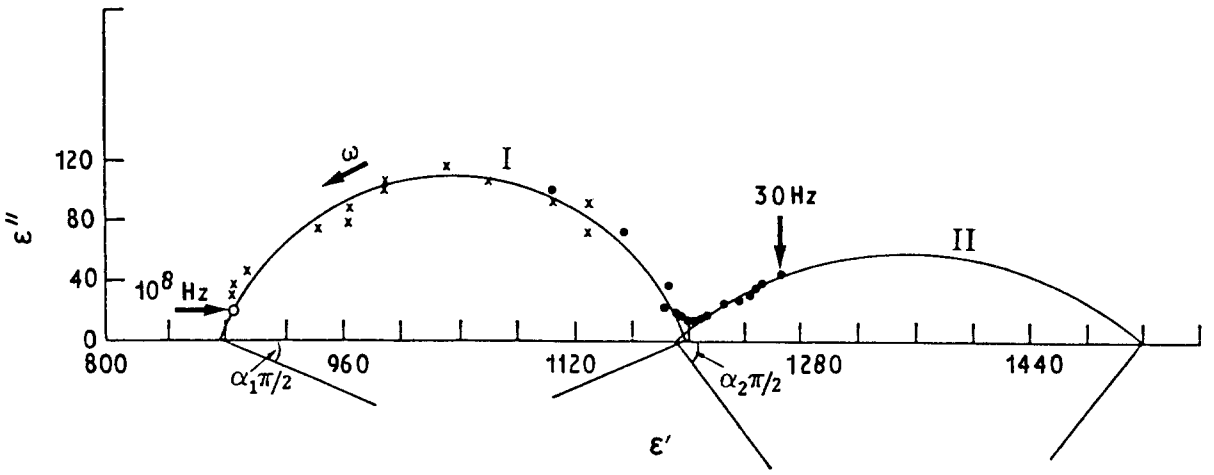

Figure 4 Cole–Cole plot for ZnO, $T = 22\,^{\circ}C$ Arc I is reproduced from [3]; Arc II is reproduced from [16].

τ_k. The total a.c. conductivity, σ_N, can then be evaluated from Equation 9.

4. The equivalent circuit of a ZnO varistor

An equivalent circuit was derived for ZnO-based ceramic varistors using the approach outlined in Sections 2 and 3.

The data available, in the literature, for ZnO-based ceramic lie in the low electric-field range [3]. They originate from different methods of measurements as illustrated in Fig. 4 for the ε''–ε' relation where two arcs are generated [16]. Detailed account of data analysis in terms of multiple-arc method is reported elsewhere [15, 16]. The arcs are characterized by the following parameters [16]:

$$\varepsilon_{sI} = 1195.0,\ \varepsilon_{\infty I} = 875.0,\ \tau_{oI} = 6.78 \times 10^{-7}\,s,$$
$$\alpha_I = 0.233;$$
$$\varepsilon_{sII} = 1507.0,\ \varepsilon_{\infty II} = 1185.0,\ \tau_{oII} = 65.78 \times 10^{-3}\,s,$$
$$\alpha_{II} = 0.555.$$

The almost non-overlapping feature of the arcs is also reflected in the corresponding RTD as evaluated by Equation 5 and depicted in Fig. 5. The effective u-range is considered to be from -16 to $+16$, corresponding to τ from 7.39×10^{-9}–5.83×10^{5} s, respectively. In order to compare σ_M with σ_N, σ_M is reproduced using Equations 2 and 6, together with the relation $\sigma = \omega\varepsilon''$.

As ε_k evaluation requires the substitution of a value for σ_M at a particular frequency, there are no direct and explicit rules for the selection of an appropriate value for σ_M at a specified τ_k. Such a selection is therefore regarded as subject to test through different schemes, with the ultimate objective of achieving the best correspondence between σ_M and σ_N. Using σ_M at $\omega = 1/\tau_k$ led to σ_N being lower by more than an order of magnitude over a wide range of frequency. On the other hand, substituting for points at $\omega > 1/\tau_k$ resulted in a similar divergence but in the lower part of the frequency range. Similarly, by using points at $\omega < 1/\tau_k$ the deviation occurred in the upper part of the range. However, from these tests, a different procedure of point selection has been devised, as outlined below.

The effective range of u from -16 to $+16$ was divided into eight blocks, each having 40 points. The block was then divided into two sections. The selection was subsequently made through an interchanging procedure whereby the points in one section are substituted for τ_k values corresponding to the other section, with the upper most value being interchanged symmetrically with the lowest point in the block. By this procedure a satisfactory convergence of σ_N to σ_M was realized, as illustrated in Fig. 6, where network and measured resistivities are compared. Satisfactory agreement is almost obtained in comparing network and measured parallel dielectric constants, as shown in Fig. 7. It is worth pointing out that although the effective range has been represented by 320 points, less than 160 branches were sufficient to simulate the dielectric characteristics over the frequency range from 30 Hz–10 MHz, as indicated in Figs 6 and 7. The values of capacitance and resistance for each of the 160 branches are shown in Fig. 8 in terms of u with τ ranging from 7.39×10^{-9}–65.67×10^{-3} s. These values are normalized to unit cross-sectional area and unit length of the ZnO-based ceramic sample. However, throughout this scheme of work, the u-domain

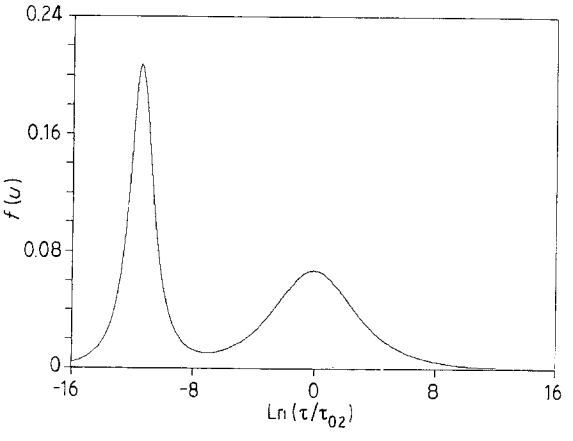

Figure 5 Relaxation time distribution for a ZnO varistor.

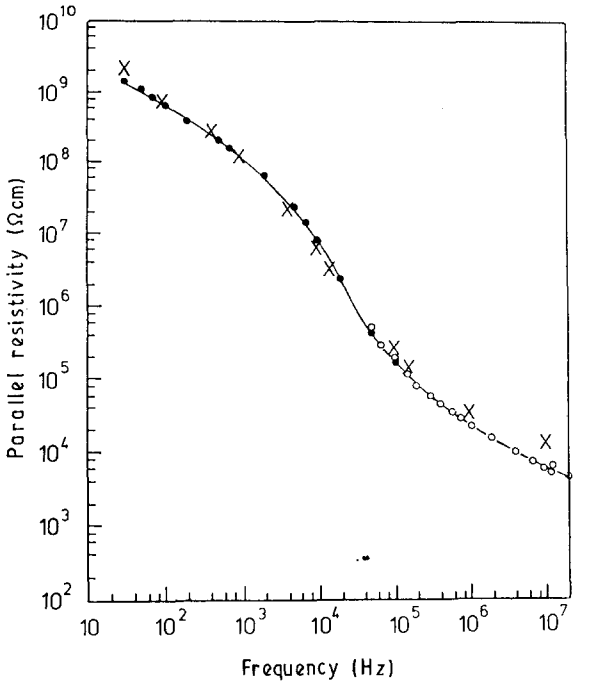

Figure 6 Comparison between measured and computed parallel resistivities. (●, ○) Reported measurements from [3], (——) reported best fit to measurements [3], (×) computed from the equivalent network.

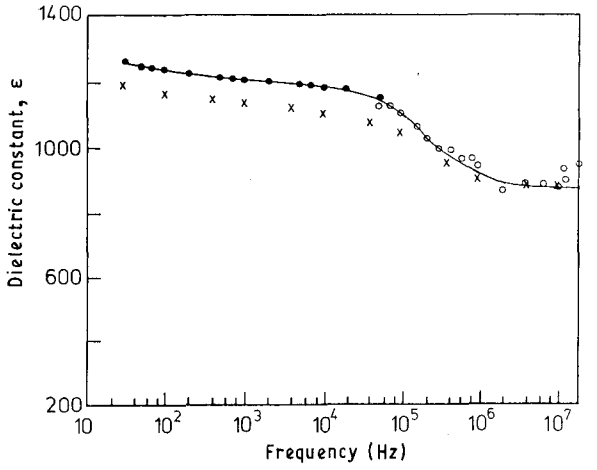

Figure 7 Comparison between measured and computed parallel dielectric constants. (●, ○) Reported measurement from [3], (——) reported best fit to measurements [3], (×) computed from the equivalent network.

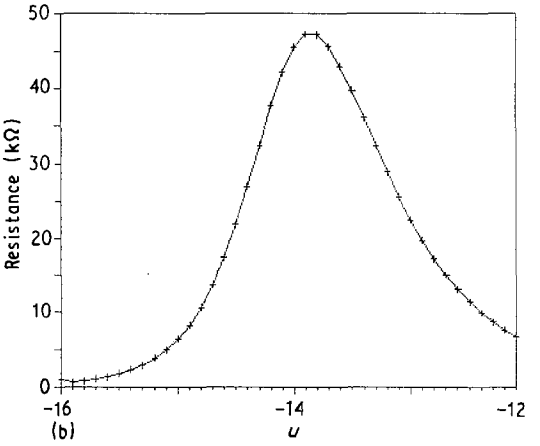

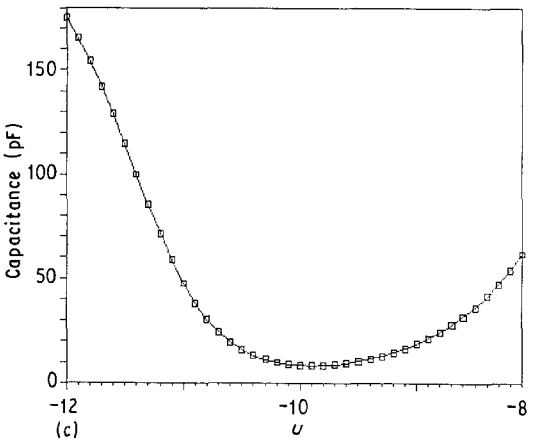

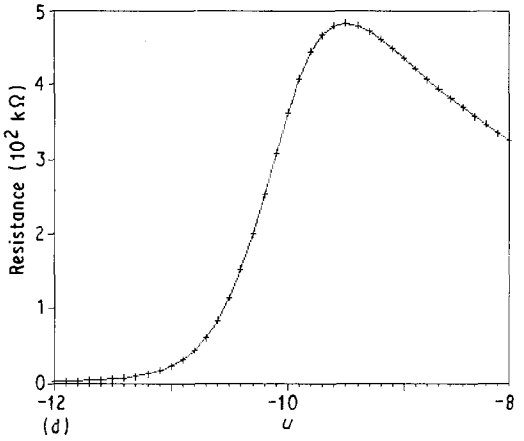

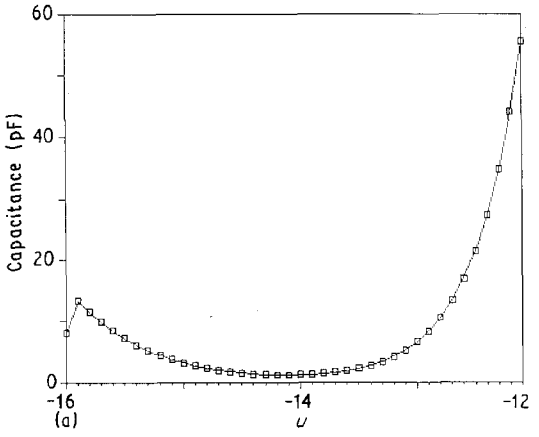

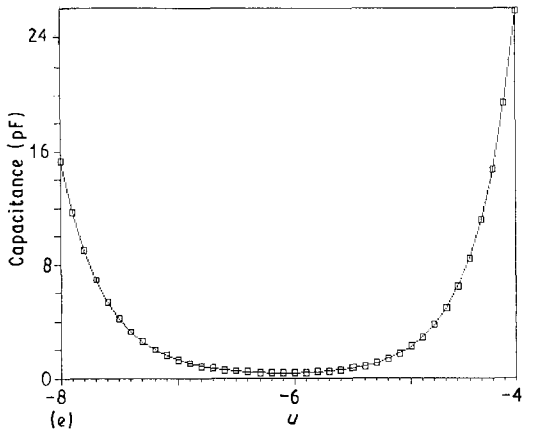

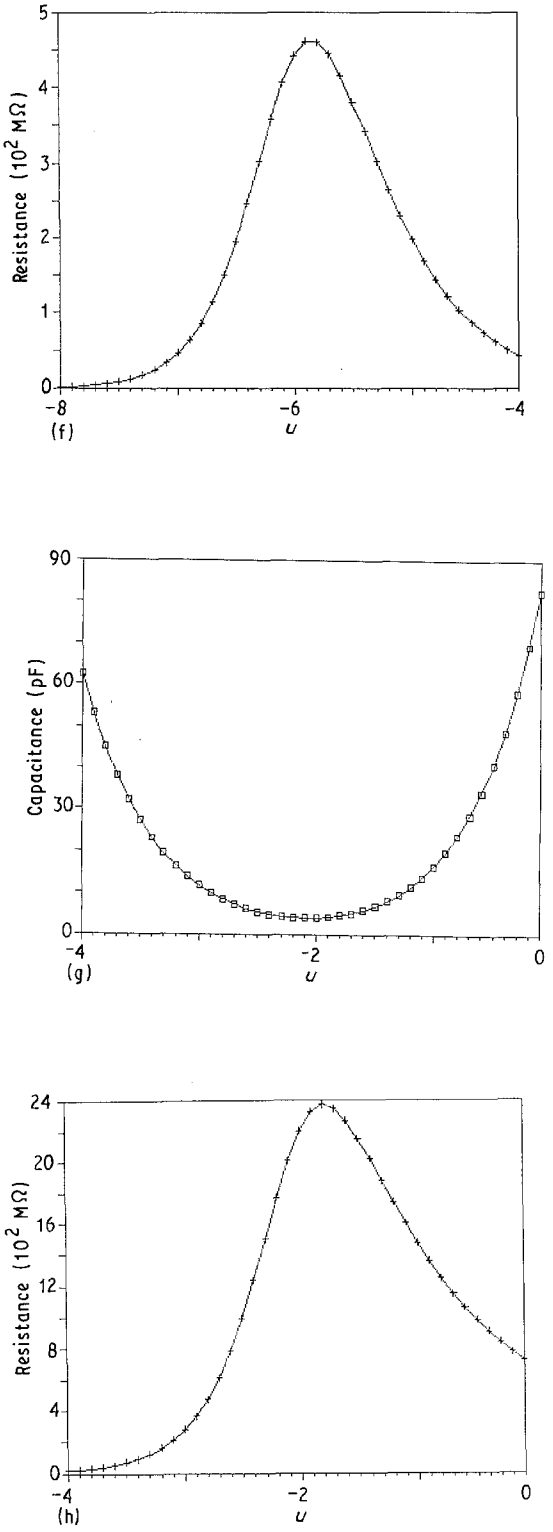

Figure 8 The values of capacitance and resistance for 160 branches computed from the equivalent network as a function of u ranging from -16 to 0. $u = \ln(\tau/\tau_{o2})$, $\tau_{o2} = 65.67 \times 10^{-3}$ s. (a, c, e, g) Capacitance values, (b, d, f, h) resistance values.

has been employed to minimize computing time. Hence the algorithm is open for further developments and optimizations through, for instance, the τ- or ω-domains.

5. Conclusion

A novel approach has been presented to derive the equivalent circuit for dielectrics. This was facilitated through multiple-arc analysis of the complex dielectric constant whereby the relaxation time distribution is correlated with the components of the dielectric equivalent circuit. The new method is then applied to the data of ZnO-based ceramic, at a low electric field. An equivalent circuit was subsequently derived with 160 parallel branches, each consisting of a simple resistance–capacitance elements connected in series. The measured a.c. resistivity and permittivity agreed satisfactorily with those derived from the equivalent network over the frequency range 30 Hz–10 MHz. The algorithm of point substitution adopted in this work can be explored further to achieve better agreement over a wider range of frequency.

References

1. A. R. VON HIPPEL, "Dielectric and Waves" (MIT, Wiley, New York, 1966).
2. P. R. EMTAGE, *J. Appl. Phys.* **48** (1977) 4372.
3. L. M. LEVINSON and H. R. PHILIPP, *ibid.* **47** (1976) 1117.
4. M. D. MIGAHED, F. M. REICHA, M. ISHRA and M. EL-NIMER, *J. Mater. Sci. Mater. Electron.* **2** (1991) 146.
5. P. J. CLARKE, A. K. RAY, J. TSIBOUKLIS and A. R. WERNINCK, *ibid.* **2** (1991) 18.
6. M. BAHAGAVENTHA REDDY and P. VENUGOPAL REDDY, *J. Phys. D. Appl. Phys.* **24** (1991) 975.
7. B. K. KUANR, P. K. SINGH, P. KISHAN, N. KUMAR, S. L. N. RAO, PRABHAT K. SINGH and G. P. SRIVASTAVA, *J. Appl. Phys.* **63** (1988) 3780.
8. P. V. REDDY, *ibid.* **63** (1988) 3783.
9. A. HADDAD, J. FUENTES-ROSADO, D. M. GERMAN and R. T. WATERS, *IEE Proc.* **137** (1990) 269.
10. A. HADDAD, H. S. B. ELAYYAN, D. M. GERMAN and R. T. WATERS, *ibid.* **138** (1991) 265.
11. A. E. FALK, B. M. LACQUET and P. L. SWART, *Electron. Lett.* **28** (1992) 166.
12. KAZUO EDA, *J. Appl. Phys.* **49** (1978) 2964.
13. V. V. DANIAL, "Dielectric Relaxation" (Academic Press, New York, 1967) Chs 2 and 5.
14. S. N. AL-REFAIE, *Appl. Phys.* **A51** (1990) 419.
15. *Idem, ibid.* **A52** (1991) 234.
16. V. V. DANIEL, *J. Mater. Sci. Lett.* **11** (1992) 988.
17. K. S. COLE and R. H. COLE, *J. Chem. Phys.* **9** (1941) 341.
18. R. M. FUOSS and J. G. KIRKWOOD, *J. Amer. Chem. Soc.* **63** (1941) 385.

Received 24 March
and accepted 14 May 1992